

Time-domain UWB RFID tag based on Reflection Amplifier

A. Lazaro, *Member, IEEE*, A. Ramos, R. Villarino, D. Girbau, *Member, IEEE*

Abstract—This work describes an active ultra-wideband (UWB) tag for radio frequency identification (RFID) and wireless sensor applications. The tag is composed by a UWB antenna connected to a one port reflection amplifier. A UWB impulse radar is used as the reader. The reader sends a short pulse and its echo is amplified and reflected back due to the return gain of the tag amplifier. The amplitude of the reflected pulse is modulated by controlling the amplifier bias. The basic theory of ultra-wideband operation applied to the time-domain RFID system is described. Experimental results with a proof of concept tag using commercial components are presented.

Index Terms—RFID, UWB, reflection amplifier, transponder

I. INTRODUCTION

Ultra-wideband (UWB) radios have relative bandwidths larger than 20%, or absolute bandwidths larger than 500 MHz [1]. Such wide bandwidths offer a wealth of advantages for both communications and radar applications. UWB tags for Radiofrequency Identification (RFID) systems have been proposed as an alternative for low-cost item tagging, [2-5]. Printable chipless RFID tags based on multiresonators in which the information is coded in frequency domain have been reported in [3-4]. An alternative method where the information is coded in time delay has been proposed in [5-6]. However, the range and number of bits suitable to be coded is limited [6]. Such networks combine low to medium rate communications with positioning capabilities. Moreover, several UWB localization systems for different applications in recent years such as emergency rescuing, patient tracking, asset or livestock tracking, etc have been suggested. UWB signaling is especially suitable in this context because of several reasons such as: the high accuracy of the range measurements achieved (order of cm), the low-power consumption and low-cost implementation of the communication systems [1]. Some of these requirements are especially desirable on many applications such as inventory items, smart sensors or surveillance systems, in which the tags must be very simple (low cost), reach long range, and have low power consumption. In order to reduce the complexity of the tag, a novel active UWB reflector is presented in this work. The goal is to increase the radar cross section (RCS) of the tag by providing gain to it. To this end, a one port

Manuscript received October 23, 2012. This work was supported by the Spanish Government Project TEC2011-28357-C02-01. A. Lazaro, A. Ramos, R. Villarino and D. Girbau are with the Electronics, Electrical and Automatics Engineering Department, Universitat Rovira i Virgili, 43007 Tarragona, Spain (antonioramon.lazaro@urv.cat, phone: +34-977.55.86.68).

reflection amplifier is connected to the tag antenna. This approach has been previously proposed for narrow-band RFID transponders [7], but it has not been explored for UWB RFID systems.

The paper is organized as follows. Section II describes the system architecture, the basic theory of operation and the implementation of an active tag based on a reflection amplifier. Section III presents the experimental results and, finally, Section IV draws the conclusions.

II. SYSTEM DESIGN

A. System description and theory of operation

The RFID system is proposed in Fig. 1. It comprises the reader and the tags. The reader interrogates the tag using a UHF (868 MHz) link, which awakes the tag logic circuitry. This signal is modulated using an OOK PWM schema in order to prevent false wake-ups due to other UHF communication systems near the tag. This work uses the TimeOn P400 MRM UWB radar for the UWB link. This radar complies with FCC regulation and sends a UWB pulse centered at 4.3 GHz with a bandwidth of 1.35 GHz and duration of 2 ns. The sampling rate of the radar is 16 GHz. The reader is connected to two UWB Vivaldi antennas.

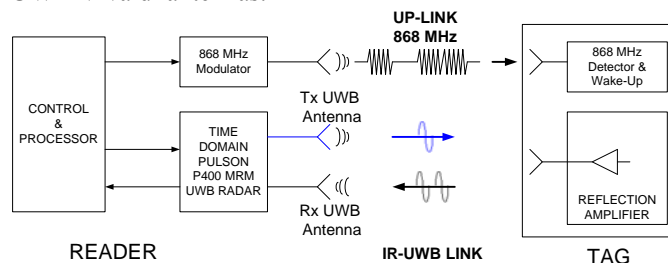


Fig. 1. UWB/UHF hybrid RFID system with UHF up-link and IR-UWB link.

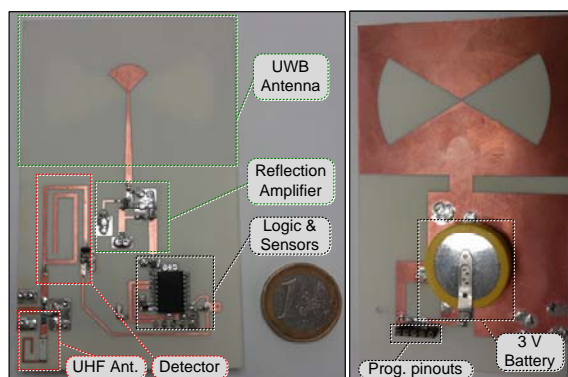


Fig. 2. Photograph of the implemented tag, front (left) and back (right).

The tag logic is composed by a PIC 16F1827 microcontroller from Microchip, which demodulates the wake-up PWM UHF signal detected by a Schottky diode detector. Then, the microcontroller acts over a MAX4715 switch from Maxim, which biases on or off the tag amplifier, in order to code a '0' or a '1' bit state. After, the reader sends an UWB pulse and receives the reflected pulse whose amplitude is modulated by the tag. Then, the reader sends an acknowledgment identifier via the UHF channel. Finally, the tag modulates the next bit. This procedure is repeated until the last bit has been received. This system, therefore, does not require implementing any synchronization mechanism between the tag and the reader. A commercial sensor can also be connected to the microcontroller, so the information responded by the tag could also be a reading from this sensor. The tag size is 63.2 mm width x 103.6 mm height.

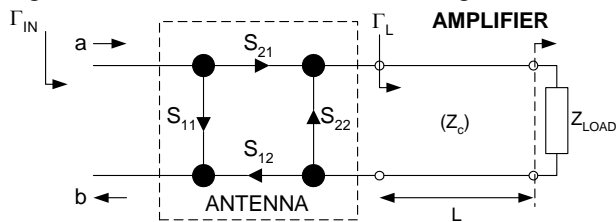


Fig. 3. Model for the UWB RFID tag.

The basic theory for time-coded chipless tags has been described in [6]. When the transmitted pulse hits the tag antenna, a portion of the electromagnetic power is backscattered towards the receiver and a portion is propagated inside the tag. Then, time-coded tags act like scattering antennas (antennas terminated with the load impedance) with two scattering modes: the structural mode (first or early-time reflection) and the tag (or antenna) mode (second reflection) can be considered. Figure 3 shows the tag which is modeled as an equivalent two-port network (antenna) terminated with a transmission line of length L and a characteristic impedance Z_c , which is in turn loaded with an impedance Z_{LOAD} . In this case, the load impedance corresponds to an output impedance of the one-port reflection amplifier ($\Gamma_{LOAD} = \Gamma_{IN,AMP}$). The wave a is the incoming wave from the radar transmitting antenna. The outgoing wave b is generated from the reflection and it is scattered towards the direction of the radar receiving antenna. Both waves are normalized to the free-space impedance ($120\pi \Omega$). The output of the antenna is normalized to Z_c . Thus, S_{22} in Fig. 3 is the reflection coefficient of the antenna. The reflection coefficient at the input of the tag Γ_{in} can be obtained from the analysis of Fig. 3 and can be approximated considering the first two reflections as [6]:

$$\Gamma_{in}(f) = S_{11} + S_{21}S_{12}\Gamma_L \left[1 + \sum_{n=1}^{\infty} (\Gamma_a \Gamma_L)^n \right] \approx S_{11} + S_{21}S_{12}\Gamma_L \quad (4)$$

Assuming a low-loss line, Γ_L can be written as $\Gamma_L = e^{-j2\pi f 2L/v} \Gamma_{LOAD}$ (v is the wave propagation velocity in the transmission line). The reflected pulse, $r(t)$, can be obtained from the inverse Fourier transform of (4):

$$r(t) = \Im(\Gamma_{IN}(f)P(f)) = p(t) * \Gamma_{IN}(t) \quad (5)$$

Where $p(t)$ is the pulse at the input of the tag, $P(f)$ its Fourier transform and $\Gamma_{IN}(t)$ is the inverse Fourier transform of the reflection coefficient given by (4).

The term S_{11} in (4) represents the structural mode, which depends on the antenna's shape, size and material and does not depend on the radiation properties of the antenna. The approximated term $S_{21}S_{12}\Gamma_L$ in (4) represents the tag mode first reflection and depends on the load connected to the antenna. From (4), infinite tag mode reflections would appear, but in practice they are quickly vanished due to the power losses in each reflection. For a UWB antenna due to its broadband operation, the S-parameters have a finite duration in time-domain. Hence, it is possible to separate the structural mode from the tag mode reflections. The tag mode occurs every $2L/v$ seconds due to the transmission line delay.

In time-coded chipless RFID, the identification for each tag is coded in the delay between the structural mode and the first reflection of the tag mode, which is approximately $2L/v$.

In our case, since the transmission line is loaded with an active amplifier, the information can be coded from the modulation of the load reflection coefficient, looking at the level of the tag mode. Therefore when the amplifier is turned off, it presents a mismatched load impedance, and $|\Gamma_{LOAD}|$ is close to 1. On the other hand, when the amplifier is turned on, it presents a negative resistance and $|\Gamma_{LOAD}| > 1$. In addition, this fact can also be used to improve the detection. Usually structural to tag mode ratios are small in time-coded chipless designs, mainly because the designers have not control over the structural mode. In this work, this poor ratio is mitigated by using the amplifier return gain. From (4) it is evident that the shape of the reflected pulse due to structural mode (S_{11}) and the tag mode is different and it is distorted by the antenna and amplifier. The Continuous Wavelet Transform (CWT) is used as a detection technique, working as a matched filter [6]. The benefit of this technique is that a template signal is not required in advance. The difficulty to detect the scattered signal and the time-of-flight in presence of noise is demonstrated using this processing technique [6].

B. Reflection amplifier

A block diagram of a one port negative resistance amplifier is shown in Fig. 4. To obtain reflection gain, the reflection coefficient of a one port network must be greater than 1, $|\Gamma_{IN,AMP}| > 1$. In this case the amplifier ought to present negative impedance at its input. The condition for a stable oscillation is $\Gamma_{IN,AMP} \cdot \Gamma_S > 1$. In this article, the reflection gain is conditioned by the return losses of the amplifier (antenna) that should be higher than the amplifier reflection coefficient. Moreover, in this case the spurious oscillations are damped.

The wideband one port reflection amplifier is designed using a small signal MESFET CFY30 from Infineon. The transistor is biased to $V_{DS}=3$ V and $I_{DS}=6$ mA. The DC power consumption is 18 mW. A source capacitor and an open stub provide positive feedback to the transistor to generate negative resistance at the operation frequency. The transistor is biased

using the source bias technique. In order to obtain the negative bias point for the V_{GS} , a 150Ω resistance is connected to the source through a high impedance $\lambda/4$ microstrip transmission line (being λ the wavelength in that medium), and the gate is grounded using a high value resistance ($20 \text{ k}\Omega$) acting as a RF chock. The 100 pF source decoupling capacitors are required to ensure that there is no RF power loss on the source resistance. A 39 nH RF chock connected to the drain presents a high impedance at RF signal and isolates the drain from the DC bias network. In order to tune the frequency of the peak gain at the center frequency of the reader's UWB pulse generator, a 1.5 pF capacitor is connected at the end of the stub. A DC blocking 10 pF capacitor is connected at the output line. The reflection amplifier is fabricated on a Rogers RO4003 substrate (32 mil thickness). Fig. 5 compares the measured and simulated reflection coefficients of the amplifier. The amplifier exhibits a negative resistance from 2 to 5 GHz. Its return gain ($|S_{11}|$) at 4.5 GHz is 10.2 dB and higher than 5 dB from 3.6 to 4.8 GHz.

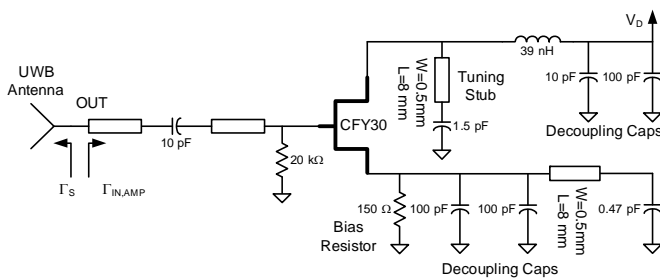


Fig. 4. Schematic reflection amplifier.

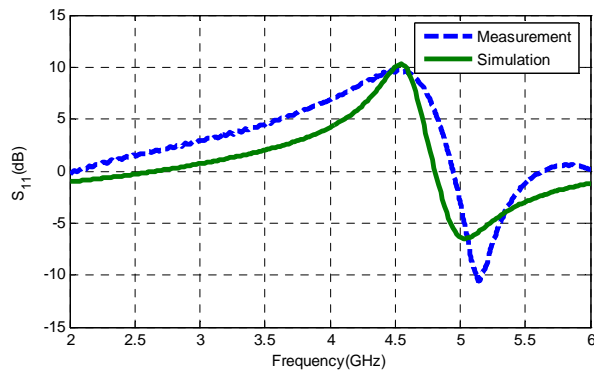


Fig.5. Comparison between measured (dashed line) and simulated (solid line) reflection coefficient of the reflection amplifier.

C. Tag antenna

The UWB antenna is based on a UWB slot bow-tie antenna similar to [8]. The shape of the slot is chosen to be radial to increase its bandwidth (the length of the slot is 26 mm and the fan angle is 60 degrees). A broadband microstrip to slotline transition based on a 8 mm length radial stub is used to feed the slot antenna. A 20 mm length microstrip taper is used to improve the matching. Compared with other microstrip fed techniques [9], this transition avoids the utilization of via holes. The antenna is designed using Agilent Momentum software. Based on the simulated results, the proposed antenna is fabricated on Rogers RO4003 substrate (thickness 32 mil).

Fig. 6 shows the antenna simulated gain and its measured

and simulated reflection coefficient. A good matching has been obtained in the 3-10 GHz band, especially around the center frequency of the UWB pulse transmitted by the radar (4.3 GHz). The gain smoothly increases from 2.5 dB to 4.8 dB between 3 and 10 GHz. In order to avoid oscillations due to the tag amplifier, the antenna return losses should be higher than 10 dB in the frequency band, where the amplifier presents gain.

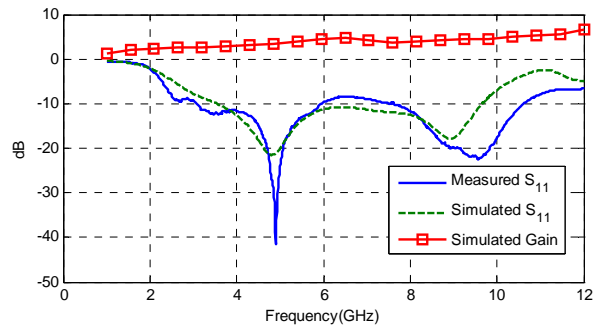


Fig. 6. Comparison between measured (solid line) and simulated (dashed line) reflection coefficient and simulated gain (squares) of the UWB antenna.

D. System link budget

In contrast with the passive UHF RFID case, the maximum read range is limited by the UWB backscattering link because of its higher attenuation than the UHF wake-up link. The read range is determined by the Bit Error Rate (BER) required, that depends on the energy per bit to noise spectral density E_b / N_0 ratio. It can be obtained from the signal-to-noise ratio (S/N) as:

$$\left(\frac{E_b}{N_0}\right)_{dB} = \left(\frac{S}{N}\right)_{dB} + P_G(dB) = 10 \log\left(\frac{S}{KT_0FB}\right) + P_G(dB) \quad (5)$$

where P_G is the processing gain ($P_G=10\log_{10}(B \cdot N_s/\text{PRF})$), F is the radar noise factor (5.8 dB), K is the Boltzmann constant ($1.38 \cdot 10^{-23} \text{ JK}^{-1}$), B is the pulse bandwidth, PRF the pulse repetition frequency and N_s the number of integrated pulses. $N_s=4096$ is considered here. The power of the signal S backscattered at the reader can be approximated by the radar equation at the center frequency of the radar (4.3 GHz):

$$S = \frac{P_t}{4\pi r^2} G_{tx} \sigma \frac{1}{4\pi r^2} \frac{\lambda^2}{4\pi} G_{rx} \quad (6)$$

where P_t is the reader transmitted power (-14.5 dBm), λ is the wavelength, G_{tx} and G_{rx} are the reader transmitting and receiving antennas gains (6 dB in our case), respectively, and r is the tag to reader distance. As it will be described in the next section a differential coding schema will be used to remove the effect of clutter and the structural mode. So the differential radar cross section (RCS) between the amplifier on and off states, σ_{dif} , associated to the differential antenna mode is estimated as:

$$\sigma_{dif} = \frac{\lambda^2}{4\pi} G_{tag}^2 |\Gamma_{in,on} - \Gamma_{in,off}|^2 \quad (7)$$

where G_{tag} is the gain of the UWB tag antenna (3 dB here). Fig. 7 has been obtained using (5)-(7). The read range for a

BER below 10^{-4} ($E_b/N_0 < 8.3$ dB) would be 11.5 m and 7.6 m for an active tag and for a passive tag (without the amplifier), respectively. The improvement in the read range is clear.

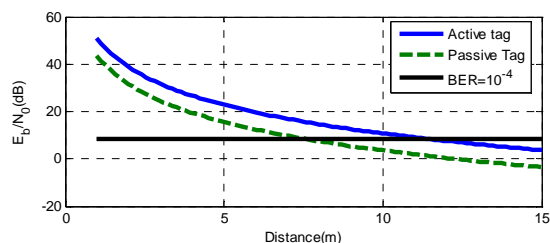


Fig. 7. Energy per bit to noise spectral density as a function of distance for an active tag and a passive tag.

III. EXPERIMENTAL RESULTS

In order to validate the design, some experiments have been performed. Fig. 8 shows the normalized magnitude of the CWT of the received signal for the state on (amplifier biased on) and off (amplifier biased off). The tag-to-reader distance is 1 m and the background (scene signal without the presence of the tag) has been subtracted from the received signal in order to remove clutter interference. The first peak corresponds to the structural mode and obviously there is no dependence between the states of the amplifier. On the other hand the amplitude of the tag mode is notably higher in the state on than in the state off, due to the return gain of the amplifier. The delay corresponds to the transmission line between the antenna and the amplifier. The ratio of the tag mode peak between the on and off states corresponds to 2.3 (7.23 dB), which agrees with the peak gain of the amplifier given in Fig. 5 at 4.3 GHz (center frequency of the radar). It is difficult to distinguish the antenna mode from the noise floor for the state off, whereas it is clearly visible (and also its own multiple reflections every $2L/v$ seconds) for the state on. Fig. 9 shows the maximum magnitude of the CWT for a bit sequence in an indoor scenario at 10 m, a value which is close to the theoretical limit for a free-space scenario (11.5 m). Since the structural-tag modes delays depend on the tag-to-reader distance, localization algorithms could use the delay information to determine the tag position using multiple readers. Assuming that clutter is stationary, its interference can be removed by subtracting a reference measurement. Fig. 9 (bottom) shows the differential signal taking the received signal for the first bit as the reference signal. It can be seen that the structural mode is cancelled and the clutter is considerably reduced.

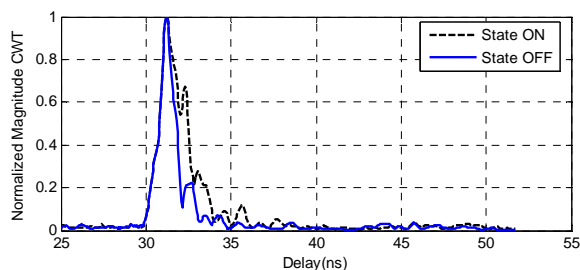


Fig. 8. Normalized CWT magnitude for the two tag states at 1 m between the tag and the reader.

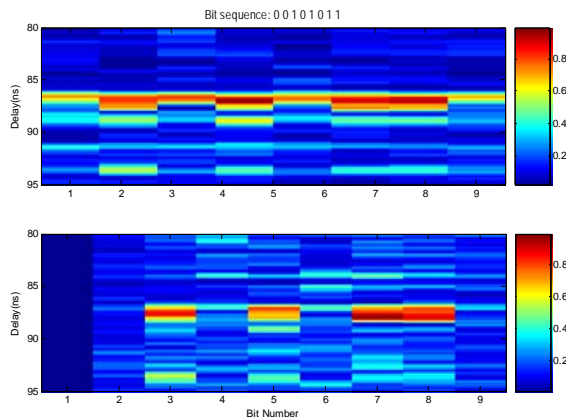


Fig. 9. Normalized CWT magnitudes (top) and differential signal (bottom) at 10 m. The first bit is the reference for the differential signal.

IV. CONCLUSION

In this work, the basic theory of operation of time-coded UWB RFID systems based on a one-port reflection amplifier is presented. A proof of concept using a novel hybrid UWB-UHF RFID system is described. The UHF link is used by the reader to awake the tag and send an acknowledge identifier. The active reflector is used to modulate the UWB pulse sent by the reader, which is amplified and retransmitted back to the reader. An experimental setup based on a UWB commercial radar is used as the RFID reader. Since the scattered signal and its time-of-flight detection in presence of noise is difficult, a Continuous Wavelet Transform working as a matched is used as a detection technique. The advantage of this technique is that a template signal is not required in advance. Indoor experimental results up to 10 m have been performed to show the viability of the system.

REFERENCES

- [1] S. Gezici, T. Zhi, G. B. Giannakis, H. Kobayashi, A. F. Molisch, H. V. Poor, and Z. Sahinoglu, "Localization via ultra-wideband radios: a look at positioning aspects for future sensor networks," *IEEE Signal Processing Magazine*, Vol. 22, No. 4, pp 70-84, Jul. 2005.
- [2] D. Dardari and R. D'Errico, "Passive Ultrawide Bandwidth RFID," *IEEE Global Telecommunications Conf. (GLOBECOM)*, pp. 1-6, 2008.
- [3] S. Preradovic, I. Balbin, N. Chandra Karmakar, and G. F. Swiegers, "Multiresonator-Based Chipless RFID System for Low-Cost Item Tracking," *IEEE Trans. On Microwave Theory and Tech.*, Vol. 57, No. 5, pp. 1411-1419, May 2009.
- [4] A. Vena, E. Perret, and S. Tedjini, "Chipless RFID Tag Using Hybrid Coding Technique," *IEEE Trans. On Microwave Theory and Tech.*, Vol. 59, No. 12, pp. 3356-3364, Dec. 2011.
- [5] S. Hu, Y. Zhou, C. L. Law, and W. Dou, "Study of a Uniplanar Monopole Antenna for Passive Chipless UWB-RFID Localization System," *IEEE Trans. On Antennas and Prop.*, Vol. 58, No. 2, pp. 271-278, Feb. 2010.
- [6] A. Lazaro, A. Ramos, D. Girbau, and R. Villarino, "Chipless UWB RFID tag detection using Continuous Wavelet Transform," *IEEE Antennas and Wireless Prop. Letters*, Vol. 10, pp. 520-523, 2011.
- [7] P. Chan and V. Fusco, "Bi-Static 5.8 GHz RFID Range Enhancement using Retrodirective techniques," *Proc. Of the 41st European Microwave Conf.*, pp. 976-979, Oct. 2011.
- [8] A. Mehdipour, K. Mohammadpour-Aghdam, R. Faraji-Dana, and A. R. Sebak, "Modified slot bow-tie antenna for UWB applications," *Microwave and Optical Technology Letters*, Vol. 50, No. 2, pp. 429-432, Feb. 2008.